This article has been accepted for inclusion in a future issue of this journal. Content is final as presented, with the exception of pagination.

Shared Control Design of a Walking-Assistant Robot

Sin-Yi Jiang, Chen-Yang Lin, Ko-Tung Huang, and Kai-Tai Song, *Member, IEEE*

***Abstract*— This brief presents a control design for a walking-assistant robot in a complex indoor environment, such that it can assist a walking-impaired person to walk and avoid unexpected obstacles. In this design, the robot motion is a resultant of autonomous navigation and compliant motion control. The compliance motion controller allows the robot to possess passive behavior following the motion intent of the user, while the autonomous guidance gives safe navigation of the robot without colliding with any obstacles. A shared-control approach is suggested to combine the passive compliant behavior and safe guidance of the robot. When a user exerts force to the robot, the mobile platform responds to adjust the speed in compliance with the user movement. On the other hand, the autonomous navigation controller is designed to provide collision-free guidance. Using the developed shared controller, outputs of the compliance motion controller and autonomous navigation controller are fused to generate appropriate motion for the robot. In this manner, passive behavior allows the walking-assistant robot to adapt to a user's motion intent and move in compliance with user. Meanwhile, the active guidance adjusts the linear velocity and the direction of the robot in real time in response to the environmental data received from the on-board laser scanner. The developed algorithms have been implemented on a self-constructed walking-assistant robot. Experimental results validate the proposed design and demonstrate that the robot can actively avoid unexpected obstacles while move passively following the user to the destination.**

***Index Terms*— Assistive device, motion control, robot control, service robot, shared control.**

I. Introduction

THE elderly population has increased rapidly in recent years. Many elderly suffer from walking impairment due to various knee or leg problems. More importantly, many elderly cannot take care of themselves in daily life, because they lose the ability to walk. It is desirable to develop some kind of walking-help system for the elderly or walk-impaired people to assist or recover their mobility. For such purpose, various walking assistant apparatus have been developed. Most existent walking assistant apparatuses are passive walkers [1]–[3]. These passive walking helpers have good support for users' body and are intrinsically safe. Recently, several passive walkers have been reported to have more advanced features. The robot walking helper i-go [4], [5] uses a braking control law on wheels to differentially steer a walking helper. However, these passive-type walkers are not sufficient for walking on slope surfaces.

On the other hand, active-type walking helpers are gaining increasing attention with various interface and control functions. These walking helpers are powered by electrical motors, and various sensors are provided to detect the user's motion intent [6]–[16]. Furthermore, active-type walking helpers can guide the user autonomously to an assigned place. The Care-O-bot II [6], [7] uses an adaptive guidance method that maintains the robot heading to the target while at the same time considering the force input of the user. The personal aid for mobility and monitoring system [8]–[10] has functions of walking assistance, navigation, and health monitoring. In [11] and [12], an active omnidirectional walking helper is presented to guide the user to avoid obstacles on the route to the target place. Mou *et al.* [13] designed a context-aware-assisted active robotic walker for Parkinson's disease patients. Wakita *et al.* [14] present dynamic models and an online inference algorithm to detect the human walking intention for an omnidirectional cane robot to assist human walking. In our previous work, an omnidirectional mobile platform has been developed for a walking-assistant robot [15], [16].

A key issue for robot-assisted walking is to provide safe and smooth motion for a user, who is weakened in self-mobility. The robotic system, while following the motion intent of the user to make the user feel as if he/she is handling a passive apparatus for walk assistance, it should actively adapt to environment autonomously on the way to a goal position. It deserves urgent attention to make the robot understand user's intention and generate proper guidance command for the walking-assistant robot in a safe manner.

A shared-control system features to combine a human user and an autonomous agent by taking advantage of the intelligence of human and the agent and to aid each other [17]. Zeng *et al.* [18] presented a collaborative wheelchair assistant method that guides the wheelchair along software-defined guide paths. Vanhooydonck *et al.* [19] proposed an adaptable navigational assistance method for intelligent wheelchairs, which continuously estimates the user's intention and determines whether the user needs assistance to achieve that intention. Carlson and Demiris [20] proposed a collaborative control method for a robotic wheelchair that system predicts the driver's intentions and adjusts the control signals to achieve the desired goal. Xu *et al.* [21] proposed a shared-control method by using a reinforcement learning algorithm for a walking-aid robot. The learning-based shared-control design allows the robot to adapt to user's individual characteristics and walking behaviors. For practical applications, it is desired to provide a design methodology to generate suitable cooperative weights

Manuscript received May 26, 2016; revised September 19, 2016; accepted November 27, 2016. Manuscript received in final form December 6, 2016. This work was supported by the Ministry of Science and Technology, Taiwan, under Grant NSC-99-2221-E-009-144. Recommended by Associate Editor M. Zefran.

The authors are with the Institute of Electrical Control Engineering, National Chiao Tung University, Hsinchu 300, Taiwan (e-mail: ktsong@mail.nctu.edu.tw).

Color versions of one or more of the figures in this brief are available online at http://ieeexplore.ieee.org.

Digital Object Identifier 10.1109/TCST.2016.2638879

1063-6536 © 2017 IEEE. Personal use is permitted, but republication/redistribution requires IEEE permission.
See http://www.ieee.org/publications_standards/publications/rights/index.html for more information.

This article has been accepted for inclusion in a future issue of this journal. Content is final as presented, with the exception of pagination.

for human and robot for the shared control to give smooth motion in walking assistance.

In this brief, we propose a shared-control scheme for a walking-assistant robot, which allows a powered robotic platform to incorporate passive behaviors. The shared-control scheme is responsible to combine the navigation behavior and compliant motion, so the robot will follow the user's motion intent in compliant motion, while avoid any obstacles during traveling. A special-designed handrail provides a reliable physical support for the elderly under various walking conditions. The user motion intent is detected by using an external force observer [22] and the corresponding robot velocity can be calculated to be compliant with human motion. To cope with slope surfaces in daily life environments [23], [24], we consider the effect of gravity in the compliant controller design. For the human-robot shared control, the heading as well as speed of the robot is adjusted in response to the distance scan data received from the onboard laser scanner.

The rest of this brief is organized as follows. Section II describes the control architecture and the proposed shared-control method of the walk-assistant robot. In Section III, the compliant motion controller is presented. Section IV describes the autonomous navigation design. In Section V, the experimental results and the evaluation of the proposed method are presented. Section VI summarizes the contribution of this brief and gives directions of further research.

II. Proposed Shared-Control Algorithm

In this design, the user is actively involved in the robot-assisted movement. Therefore, a shared-control system is suggested to consider the user's motion intent and assure that the desired motion is safe. Therefore, the control action is a resultant of compliant motion and robot guidance to move toward the goal position as desired. In the shared-control design, the walking-assistant robot has two sources of motion commands: one from the autonomous navigation controller and another from the compliant motion controller. The compliant motion controller works to provide passive walking assistance, while the autonomous navigation controller adjusts robot motion to achieve the goal safely.

We combine these two controllers to generate the desired assistive mobility. The goal of the shared control is to allow the robot to perform passive assistance while aiding the user to the destination, without colliding into any obstacles on the way to the destination. Consequently, active navigation must understand the desired motion from the compliant controller. For instance, if the user slows down and stands still without exerting any force on the handrail, the controller will stop the robot due to the absence of any external force. It is clear that, when the user stops, the navigation controller should not move the robot.

The proposed control architecture of the walking-assistant robot is illustrated in Fig. 1. We see in the figure that the suggested shared controller generates the desired motion commands by fusing the output of the compliant controller and navigation controller. To do so, the user cooperative weight and robot cooperative weight are dynamically generated according to sensory data of environment configuration. The final

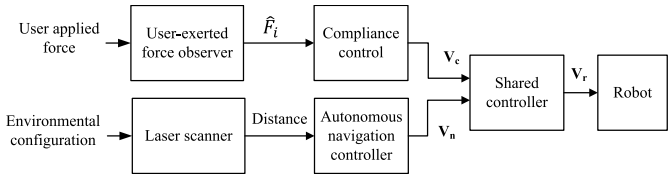

Fig. 1. System architecture of the proposed shared-control system.

velocity command of the shared-controller, V_r, is the sum of the weighted compliant motion command and the weighted autonomous navigation command

$$\mathbf{V_r} = W^u \mathbf{V_c} + W^r \mathbf{V_n} \tag{1}$$

where W^u is the user cooperative weight, W^r is the robot cooperative weight, W^u and W^r are between 0 and 1, $\mathbf{V_c}$ is the velocity command of the compliant controller, and $\mathbf{V_n}$ is the velocity command of the navigation controller.

The user cooperative weight and the robot cooperative weight should be determined online in order to maintain safe walking of the user. We consider that when the robot is compliant to the user's intent to move faster or when the robot comes close to an obstacle, the weight of compliant motion controller must decrease and the weight of navigation controller must increase to keep safe. So we take the current output of compliant controller and the distance between the robot and obstacles into account to determine suitable cooperative weights for the compliant controller and navigation controller, respectively. Consequently, two factors are considered to determine the cooperative weights. One is the user's walking velocity (i.e., the velocity commend from the compliant controller), another is the distance to the obstacles (as measured by the laser scanner).

A. Velocity Factor

In order to generate a proper cooperative weight for the navigation output, we first focus on the linear velocity of the robot. When the velocity of the robot is somehow high, the user is in a relative dangerous situation. It would be better to allow the robot autonomy to handle the motion and provide a safer walking. On the other hand, when the robot linear velocity is slow, it is safe for the user to control the robot walker following the user motion intent. The velocity factor W_v^r is determined by

$$W_v^r\left(V_c^l\right) = \frac{1}{1 + e^{-\gamma_1\left(\frac{V_c^l}{V_{c-\max}^l} - \delta_1\right)}} \tag{2}$$

where W_v^r is a value between 0 and 1 (see Fig. 2),V_c^l is the linear velocity of compliant motion control, $V_{c-\max}^l$ is the speed limit in compliant motion, and γ_1 and δ_1 are constants. When the user moves at relative high speeds, the velocity factor will increase the robot control authority while decrease the user control authority to protect the user to move in a safe motion path. For instance, due to the impaired walking, the user might impose wrong force on the robot, so that the user may move in a relatively high-speed motion. Hence, the velocity factor will increase the robot control authority

This article has been accepted for inclusion in a future issue of this journal. Content is final as presented, with the exception of pagination.

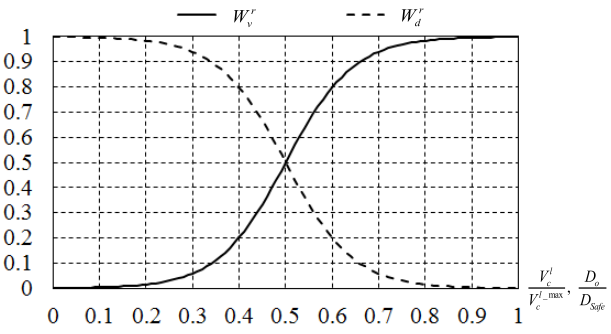

Fig. 2. Determination of cooperative weight for the velocity factor and distance factor. The horizontal axis of the velocity factor and the distance factor are normalize linear velocity V_c^l and normalize distance to obstacle D_o, respectively.

and decrease the user control authority for keeping the user walking in a safe.

The constant δ_1 determines the half-value position of W_v^r. When the input (linear velocity) is smaller than δ_1, the user will have more authority to correct the robot motion direction and the robot heading. When input (linear velocity) is greater than δ_1, the autonavigation has more authority to correct the robot motion. The constant γ_1 adjusts the magnitude of W_v^r, which allows W_v^r to change smoothly.

B. Distance Factor

We define a distance factor W_d^r to ensure the ability for a walk-assist robot to avoid an obstacle. The compliant controller has a lower cooperative weight or a smaller distance factor W_d^r when the user moves closer to any obstacle. The distance factor is determined by

$$W_d^r(D_o) = \frac{1}{1 + e^{\gamma_2\left(\frac{D_o}{D_{\text{Safe}}} - \delta_2\right)}} \tag{3}$$

where W_d^r is a value between 0 and 1 (see Fig. 2), D_o is the minimize distance between a robot and any obstacle, D_{safe} is a constant to define a safe distance, and γ_2 and δ_2 are constants. When the robot moves near to any obstacle, the distance factor will increase and thus increase the weight of robot navigation control while decrease the weight of compliant motion control to keep the user move away from any obstacles. When $D_o \geq D_{\text{safe}}$, the environment is quite open and the distance factor W_d^r is 0. On the contrary, if the robot is closer to any obstacle, the distance factor W_d^r will increase gradually to allow the navigation controller to take control of the robot.

The user cooperative weight and the robot cooperative weight are dynamically determined according to the distance factor and the velocity factor, such that

$$\begin{aligned} W^r &= \min\left(W_v^r, W_d^r\right) \\ W^u &= 1 - W^r \end{aligned} \tag{4}$$

The robot cooperative weight uses the minimum function to get a lower value. In (4), the robot control authority and user control authority are determined by the velocity factor and distance factor. The navigation controller and the compliant controller are working in cooperation to determine a proper robot motion.

III. Compliant Motion Controller

For a user to easily handle the walking-assistant robot, the robot should be designed to have passive mobility. Thus the control loop includes the force exerted by the user on the robot, so that the robot's velocity will follow the user in compliant motion. When a user exerts an external force on the walking-assistant robot, the mobile platform will respond to it by adjusting its speed.

A. Estimation of User-Exerted Force

An external force/torque estimation scheme has been developed using motor currents and angular velocities, without using costly force/torque sensors [15]. In this design, angular velocities are obtained from shaft encoders and motor currents are obtained from a current sensing device. To derive an expression of the user-exerted force on the handrail, we examine the total external force on the robot, described as

$$\mathbf{F}_{\text{ext}} = \mathbf{F}_i + \mathbf{F}_f + \mathbf{F}_g \tag{5}$$

where F_{ext} denotes the total external force, including the user's intention F_i, friction force F_f, and gravity F_g applied to the robot center. The dynamic equation of the robot is described by a mass/damper model as follows:

$$\mathbf{M}_r \cdot \dot{\mathbf{V}}_r^e + \mathbf{D}_r \cdot \mathbf{V}_r^e = \mathbf{F}_O - \mathbf{F}_{\text{ext}} \tag{6}$$

where $M_r = \text{diag}(M_r, M_r, I_z)$ and $D_r = \text{diag}(D_x, D_y, D_z)$ are the inertia and damping coefficients, respectively, of the walking-assistant robot, and $\mathbf{V}_r^e$ is robot center velocity. In this brief, we assume that the friction force, F_f, is constant in the operation. The gravity force is given in (7), which can be obtained from the mass of the robot and the slope angle of the walking surface. The roll angle α and pitch angle β of the slanted surface are used to calculate the gravity compensation. The gravity F_g that needs to be compensated is expressed as below

$$\mathbf{F}_g = \begin{bmatrix} F_{gx} \\ F_{gy} \\ 0 \end{bmatrix} = \begin{bmatrix} M_r g \sin\alpha \\ M_r g \sin\beta \\ 0 \end{bmatrix} \tag{7}$$

where M_r is the robot mass and g is the acceleration of gravity. Hence, the external force exerted by the user F_i is measured as follows:

$$\begin{aligned} \hat{\mathbf{F}}_i = &\frac{G_O\left(\mathbf{F}_O + G_O\mathbf{M}_r \cdot \mathbf{V}_r^e - \mathbf{D}_r \cdot \mathbf{V}_r^e - \mathbf{F}_f - \mathbf{F}_g\right)}{s + G_O} \\ &- G_O\mathbf{M}_r \cdot \mathbf{V}_r^e. \end{aligned} \tag{8}$$

The parameter G_O is related to the dynamics of the force estimation model, and larger G_O values will enable the observer to estimate external force faster and more stably. The force exerted on the robot body (F_O) can be obtained from the currents of the four motors. $\mathbf{V}_r^e$ can be calculated using the velocities of the four wheels, by measuring the shaft angular velocities. From (8), the external force exerted by a user can be estimated by measuring the four motor currents, shaft angular velocities, and inclined angle of the surface. For the detail description of the external force observer, please refer to [25].

This article has been accepted for inclusion in a future issue of this journal. Content is final as presented, with the exception of pagination.

B. Compliant Motion

The desired passive behavior of the walking-assistant robot is determined based on a dynamic model. This model can be considered as the desired dynamic behavior of the robotic system following the user's motion intent. Therefore, the passive behavior of whole system can be described as

$$\mathbf{M_d}\dot{\mathbf{V}}_\mathbf{c} + \mathbf{D_d}\mathbf{V_c} = -\hat{\mathbf{F}}_\mathbf{i} \tag{9}$$

where $\mathbf{M}_d$ and $\mathbf{D}_d$ are the desired virtual mass and virtual damping of the overall system, and $\mathbf{V_c}$ is the output velocity command. The velocity of compliant motion is calculated by taking the Laplace transform of the dynamic equation (9). Then the bilinear transform is applied to transform it to the Z-domain, and finally takes inverse Z transform. The velocity command of compliance motion controller is described as

$$\mathbf{V_c} = \left[\, V_l^c \;\; \omega_z^c \,\right]^\mathbf{T} \tag{10}$$

where V_l^c is linear velocity commands, and $\omega_z^\mathbf{c}$ is the angular velocity commands in robot frame. The compliance motion controller calculates the velocity of the walking-assistant robot according to the estimated exerted force. The motion control system receives the computed velocity commands and generates the actuation current in the motors of the walking-assistant robot. The parameters M_d and D_d determine the output response of the compliance controller. M_d and D_d can be adjusted to a desired passive behavior to satisfy the user's preference. A relative small M_d value gives a relative fast response and vice versa. D_d influences the output velocity magnitude of the compliance controller. A relative small D_d value gives a relative high response and vice versa. In the situation when there is a sudden change of applied force from the user, the system will not generate sudden velocity change by using a suitable virtual mass M_d. The user can keep to walk with a safe motion speed.

IV. Autonomous Navigation Controller

The navigation algorithm of the current omnidirectional mobile robot was modified from the method presented in [26]–[28]. The motion control commands are sent to motion control boards, where velocity servos of wheel motors are implemented. The measured distance from the laser scanner and robot pose are feedback to navigation controller. The navigation algorithm adjusts robot velocity to prevent from collision with obstacles on the path to the goal. In this navigation controller design, the output robot angular velocity is calculated from the inputs distance data from the laser scanner [16], [26], [27].

A SICK LMS 100 laser scanner was installed at the front of the robot to acquire obstacle distance [29]. In this design, a 180° scan is divided into nine divisions (Range 1–Range 9), with each division covering 20°. The sensor value of each division is given by the minimum range readings in that division. The detected sensor values are then grouped into group 1–group 5, including right side (Range 1 and Range 2), right front (Range 3), front (Range 4–Range 6), left front (Range 7), and left side (Range 8 and Range 9). We designed three navigation behaviors using a fuzzy logic approach. The outputs of these behaviors are fused according to fusion weights determined by a behavior-fusion scheme.

A. Obstacle-Avoidance Behavior

The obstacle avoidance behavior generates angular velocity of the robot command. Distance measurements from the laser scanner are used to determine a suitable angular velocity of the robot in order to prevent any collision with obstacles. The front-side distances of Range 4–Range 6 are used as inputs for the obstacle avoidance controller. The obstacle-avoidance behavior gives the robot angular velocity. Meanwhile, the distance data from Range 3 and Range 7 are used to determine turning right or turning left for the calculated angular velocity.

B. Wall-Following Behavior

The wall-following behavior allows the robot to move along the nearest wall by keeping a given distance to the wall. The distance difference between the right-hand side (Range 1 and Range 2) and left-hand side (Range 8 and Range 9) is taken as the input for a wall-following fuzzy logic controller (FLC). The output of the FLC is the angular velocity of the robot to keep moving along the wall. The wheel speeds are determined accordingly.

C. Goal-Seeking Behavior

Goal-seeking behavior is designed to guide the robot toward the goal. When the obstacle-avoidance or wall-following behavior is activated, the robot heading might deviate from the goal direction. Goal-seeking behavior turns the robot toward the goal. The difference between the goal direction and robot heading is set to be the input for the goal-seeking FLC. The output of the FLC is also the angular velocity of the robot.

D. Behavior Fusion

A fuzzy Kohonen clustering network (FKCN) [28] is utilized to map the environmental information to fusion weights for the above three navigation behaviors and calculates the linear velocity of the robot. The rule table and FKCN are used to generate the fusion weights of three behaviors on-line in real time during robot navigation. After receiving the distance data from laser scanner for current environmental information, the fusion weights are calculated accordingly to generate motion commands such that

$$\omega_d^n = W_O^k \cdot \omega_O^n + W_G^k \cdot \omega_G^n + W_W^k \cdot \omega_W^n \tag{11}$$

where ω_O^n, ω_G^n, and ω_W^n are, respectively, the output robot angular velocity of each behavior, and W_O^k, W_G^K, and W_W^k are, respectively, the fusion weights of each behavior. The FKCN calculates fusion weights of three behaviors and also calculates the linear velocity command of navigation controller V_l^n (please refer to [28]). Hence, the velocity command of the autonavigation controller is described as

$$\mathbf{V}_n = \left[\, V_l^n \;\; \omega_d^n \,\right]^T. \tag{12}$$

The navigation controller adjusts the robot's linear velocity and angular velocity to generate the desired robot motion.

This article has been accepted for inclusion in a future issue of this journal. Content is final as presented, with the exception of pagination.

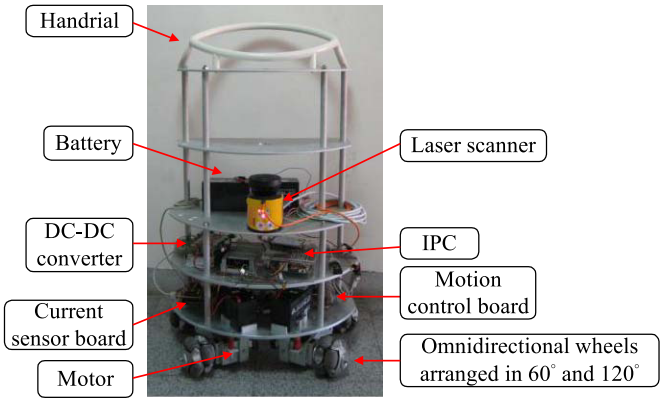

Fig. 3. Photograph of the walking-assistant robot.

Fig. 4. Experimental setup for walking assistance on a slope surface.

V. Experimental Results

A prototype walking-assistant robot (Walbot) has been designed and constructed in our laboratory for experimental study. To increase its motion capacity and consider human holonomic mobility, we adopted an omnidirectional design for the mobile platform. Fig. 3 shows a recent photo of Walbot. A handrail is provided to support the user during robot-assisted walking. Four omnidirectional wheels were arranged in 60° and 120° directions on the base of the robot platform, which has a half-moon shape so the user can handle the robot and walk easily. The laser scanner was installed in the middle of the robot for environment detection. An inertial measurement unit (IMU) was attached to the robot to measure the slope angles of ground surface.

Several interesting experiments have been carried out to verify the developed method. In this section, we first present the compliance motion control of the robot and then show the effectiveness of the shared control walking assistance in indoor environments.

A. Compliant Motion Control on Slope Surfaces

In this experiment, we validate the proposed user-exerted external force observer. Fig. 4 shows the experimental environments built in the lab with 4° uphill and downhill slopes. The parameters of the robot are as follows: mass M_r = diag (76.9, 76.9, 2.5) and damping D_r = diag (75.3, 75.3, 5.7) for the model (9). Through the external force observer and compliant

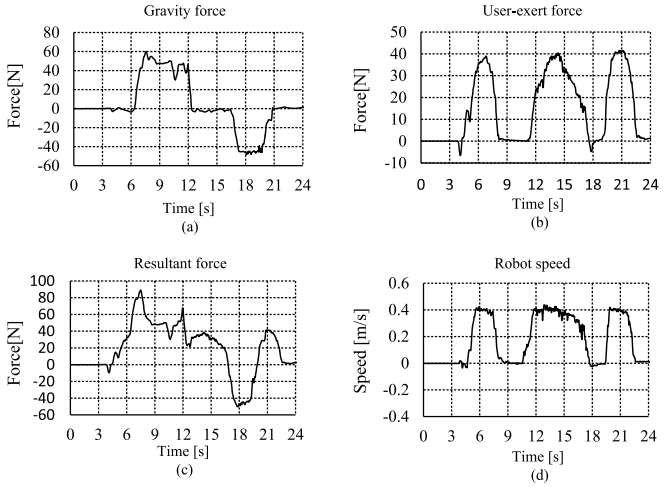

Fig. 5. Recorded responses of experiment on 4° slope surface. (a) Gravity force. (b) Estimated user-exerted force. (c) Force generated by the motors. (d) Robot speed.

motion controller, the walking-assistant robot inferred the user's motion intent and converted it to the corresponding speed commands. The roll angle α and pitch angle β of the robot were obtained by the IMU. In this experiment, we set the desired virtual mass $M_d = \text{diag}(0.1, 0.1, 1)$, with units of kg and kg-m^2, and virtual damping D_d = diag (75.3, 75.3, 6.5), with units of N$\cdot$s/m and (N$\cdot$m)$\cdot$s/rad, friction force F_f = (20.00, 25.77, 6.93), with unit of N, and G_o = 100 in the passive model of compliance controller. In this experiment, a smaller M_d value was assigned for faster response of the compliance controller. In the experiment, the user pushed the handrail of the walking-assistant robot to move on the 4° slope. The user stopped the robot on uphill between 8 and 11 s and on downhill between 17.5 and 19.5 s, as shown in Fig. 5. Fig. 5(a) shows the calculated gravity force on the walking-assistant robot. The uphill slope was detected at time instant 6 s and the gravity force was around 50 N. It can be seen in Fig. 5(b) and (c) that the gravity force was estimated correctly. The downhill slope was detected at time instant 16.5 s, and the gravity force was estimated around -50 N as expected. Fig. 5(c) shows that the force generated by the motors increased immediately to resist the gravitational force. The user's exerted force was estimated without being influenced by the gravity force on the slope. As can be seen in Fig. 5(d), the robot speeds were not influenced by the slanted surfaces.

In the second experiment, the robot cover was removed and was walked by the user on a 6° slope. After removing the robot cover, the robot mass was reduced to 40 kg. Fig. 6(a) shows the calculated gravity force on the walking-assistant robot. Because the robot has a smaller mass, the gravity force is smaller than that on 4° slope. It can be seen that the slope was detected at around 2 s and the gravity force was estimated to be 35 N, which is smaller than that of 4° slope but in accordance with the 6° slope. During time instant 4–8 s, the user stopped on the slope and released the handrail. It can be seen in Fig. 6(b) that the user exerted force reduced to 0 and in Fig. 6(c) that the resultant force is almost equal to the gravity force as expected. The robot speed was not influenced by the slanted surfaces, as shown in Fig. 6(d).

This article has been accepted for inclusion in a future issue of this journal. Content is final as presented, with the exception of pagination.

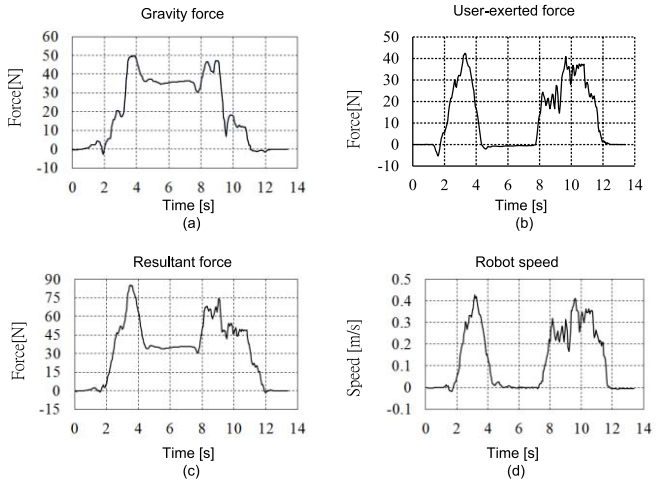

Fig. 6. Recorded responses of experiment on 6° slope surface. (a) Gravity force. (b) Estimated user-exerted force. (c) Force generated by the motors. (d) Robot speed.

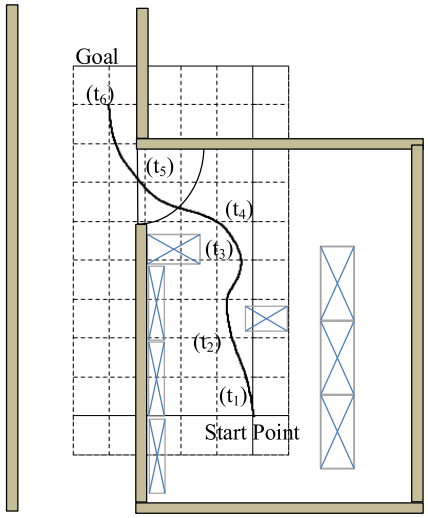

Fig. 7. Recorded trajectories of the robot in the shared-control experiments.

These experiments validate the effectiveness of the proposed external force observer and the compliant controller.

B. Shared-Control Walking Assistance

To verify the effectiveness of the shared-control design, we experimented to walk with Walbot in a room with obstacles. In the experiment, the user started from inside the lab and walked to the target in the corridor. In this experiment, we set M_d = diag (0.1, 0.1, 1), with units of kg and kg-m^2, D_d = diag (105, 105, 13), with units of N·s/m and (N·m)·s/rad, friction force F_f = (20.00, 25.77, 6.93), with unit of N, and $G_o = 100$ in the passive model of compliant controller. In this experiment, we adopted a larger virtual damping D_d for the user to walk slower in order to observe the response of shared controller.

The user walked with Walbot in the corridor to test the proposed shared controller. The parameters $\delta_1 = 0.5$, $\gamma_1 = 0.4$, $\delta_2 = 0.5$, and $\gamma_2 = 200$, which means that the robot output has more control authority when $V_c^l / V_{c-}^{l\,\max} > 0.5$ or $D_o / D_{\text{Safe}} < 0.5$. Fig. 7 shows the recorded motion trajectory of the experiment. The force responses are presented in Fig. 8(a) and (c). Fig. 8(b) and (d) shows the corresponding robot speeds in robot coordinate. It can be seen that the exerted force from the user is mainly in the forward direction. It is observed in Fig. 8(a) that in region (t_3), the robot stopped temporarily as the user stopped and did not press the handrail [Fig. 8(b)]. It can be seen that the walking-assistant robot behaved with satisfactory compliance.

Fig. 9(a) shows the robot cooperative weight W^r in the experiment. Fig. 9(b) shows the velocity factor W_v^r and the distance factor W_d^r values in this experiment. Fig. 10(a) and (b) shows the weighted autonomous navigation commands, compliant motion, and the final shared control commands of linear velocity and angular velocity, respectively. In region (t_1), the distance from obstacles are still far; therefore, the robot cooperative weight is low and the user has more authority to control, as shown in Fig. 9. The major velocity commands of the controller are from the compliant motion controller,

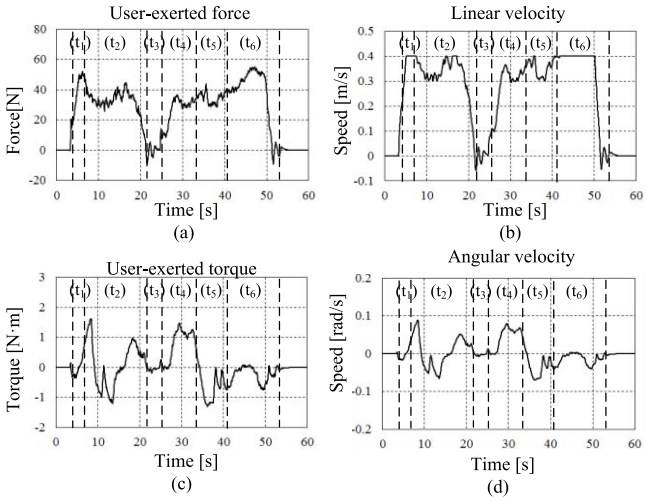

Fig. 8. Recorded forces and velocities of the robot in shared control experiment. (a) User-exerted force. (b) Linear velocity. (c) User-exerted torque. (d) Angular velocity. (t_1)–(t_6) region of this figure corresponds to the (t_1)–(t_6) region of Fig. 7.

as shown in region (t_1) in Fig. 10. The results validate the distance factor, the velocity factor, and the cooperative weights by using the proposed method.

In region (t_2), the robot moved near to obstacles. The robot autonomous control authority increases and the user control authority decreases to avoid the obstacle. The robot cooperative weight is calculated according to the environment configuration, as shown in Fig. 9. We see in Fig. 9(a) around 13 s that the robot cooperative weight changed from 0.7 to 0.3, which results from that the distance factor changed from 0.95 to 0.3, as shown in Fig. 9(b). The robot has just finished the obstacle avoidance by using the measured laser distance. It is observed that the linear velocity of shared control output increased from 0.2 to 0.25 m/s, as shown in Fig. 10(b). There is no sudden velocity change following the obstacle avoidance in this design. The user experienced a slower walking speed in obstacle avoidance then returned to normal walking speed.

This article has been accepted for inclusion in a future issue of this journal. Content is final as presented, with the exception of pagination.

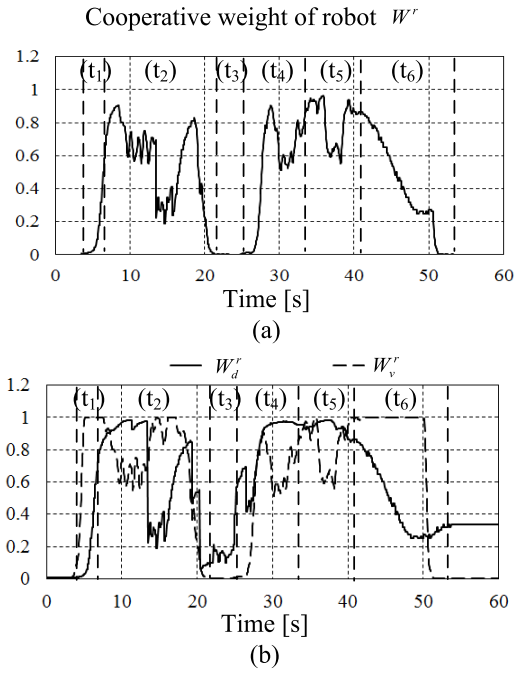

Fig. 9. (a) Recorded the robot cooperative values during the experiment. (b) Recorded distance factor and velocity factor during the experiment. (t_1)–(t_6) region of this figure corresponds to the (t_1)–(t_6) region of Fig. 7.

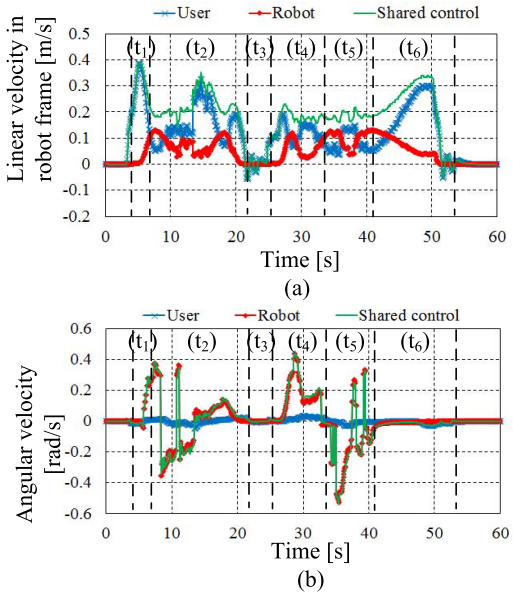

Fig. 10. (a) Recorded robot linear velocity commands of the robot frame. (b) Recorded robot angular velocity commands of the robot frame. (t_1)–(t_6) region of this figure corresponds to the (t_1)–(t_6) region of Fig. 7.

Under such a circumstance, the force applied to a user does not change suddenly. The result validates that the proposed method is safe for a user.

In region (t_3), the user stopped without exerting force on the robot. Both the velocity command of compliant motion controller and the velocity factor decrease to 0. The velocity command of shared controller is 0 and the robot cooperative weight is also 0 due to the velocity command of compliant motion controller is 0; therefore, the robot stops, as shown in Fig. 10. In regions (t_4)–(t_5), the shared controller allows the robot to avoid obstacles and to pass through a narrow doorway. The robot cooperative weight increased when the robot encountered obstacles, as shown in the region (t_4) of Fig. 9. After the user passes the doorway, the navigation controller generated a right-turn command to guide the user to the goal direction, as shown in the region (t_5) of Fig. 10(b). In region (t_6), the distance to obstacles is large, the robot control authority decreased, and the user control authority increased as the user walked in the corridor, as shown in Fig. 7. In this experiment, the robot encountered several obstacles on its way through the corridor and the shared control output response to move safely as expected. This experiment validates that the proposed shared-control guidance scheme effectively integrates both compliant and autonomous behaviors in an indoor environment. Compared with the previous results of human-robot shared control design, the proposed method provides smooth robot motion by generating appropriate cooperative weights for human and robot.

The safety of a user is essential for developing walking-assistant robots. A user must be supported by the robot during walking to prevent from fall. In the current design, by selecting suitable parameters in the model, the system will generate smooth motion without sudden velocity change during guidance even if there is a sudden change of applied force from the user. Furthermore, the proposed shared-control scheme allows the robot to prevent from any collisions from obstacles and the proposed walking-assistant robot will not endanger the safety of the user. For practical applications, the safety design of a walking-assistant robot will need to consider various user conditions, such that a velocity limit or user status monitoring can be added to ensure safety during operating the robot.

VI. Conclusion and Future Work

This brief presents a novel shared-control design for a walking-assistant robot to combine active robot navigation and passive mobility. The passive behavior allows the walking-assistant robot to adapt to user's motion intent and move in compliance with the user. Meanwhile, the active navigation adjusts the speed of the robot in real time in response to data received from the on-board laser scanner. The walking-assistant robot can follow user's motion intent, and also actively avoid any unexpected obstacles. The gravity force is estimated by the proposed force observer, such that the robot can comply with a slope surface, and the walking-assistant robot can be operated as if it were on a horizontal plane. In the future, we will continue to focus on the development smoother compliant motion in the walking-assistant guidance. User gait estimation and fall prevention will be investigated to allow the robot to react more safely under situations of fall happening.

References

[1] Y. Hirata, A. Muraki, and K. Kosuge, "Motion control of intelligent walker based on renew of estimation parameters for user state," in *Proc. IEEE/RSJ Int. Conf. Intell. Robots Syst.*, Beijing, China, Oct. 2006, pp. 1050–1055.

This article has been accepted for inclusion in a future issue of this journal. Content is final as presented, with the exception of pagination.

[2] Y. Hirata, A. Hara, and K. Kosuge, "Motion control of passive intelligent walker using servo brakes," *IEEE Trans. Robot.*, vol. 23, no. 5, pp. 981–990, Oct. 2007.

[3] J. Glover *et al.*, "A robotically augmented walker for older adults," Dept. Comput. Sci., Carnegie Mellon Univ., Pittsburgh, PA, USA, Tech. Rep. CMU-CS-03-170, 2003.

[4] C. H. Ko, K. Y. Young, Y. C. Huang, and S. K. Agrawal, "Active and passive control of walk-assist robot for outdoor guidance," *IEEE/ASME Trans. Mechatronics*, vol. 18, no. 3, pp. 1211–1220, Jun. 2013.

[5] C. H. Ko, K. Y. Young, Y. C. Huang, and S. K. Agrawal, "Walk-assist robot: A novel approach to gain selection of a braking controller using differential flatness," *IEEE Trans. Control Syst. Technol.*, vol. 21, no. 6, pp. 2299–2305, Nov. 2013.

[6] B. Graf, "An adaptive guidance system for robotic walking aids," *J. Comput. Inf. Technol.*, vol. 17, no. 1, pp. 109–120, 2009.

[7] J. M. H. Wandosell and B. Graf, "Non-holonomic navigation system of a walking-aid robot," in *Proc. IEEE Int. Workshop Robot Human Interact. Commun.*, Berlin, Germany, Sep. 2002, pp. 518–523.

[8] S. Dubowsky *et al.*, "PAMM—A robotic aid to the elderly for mobility assistance and monitoring: A 'helping-hand' for the elderly," in *Proc. IEEE Int. Conf. Robot. Autom.*, San Francisco, CA, USA, Apr. 2000, pp. 570–576.

[9] H. Yu, M. Spenko, and S. Dubowsky, "An adaptive shared control system for an intelligent mobility aid for the elderly," *Auto. Robots*, vol. 15, no. 1, pp. 53–66, 2003.

[10] M. Spenko, H. Yu, and S. Dubowsky, "Robotic personal aids for mobility and monitoring for the elderly," *IEEE Trans. Neural Syst. Rehabil. Eng.*, vol. 14, no. 3, pp. 344–351, Sep. 2006.

[11] O. Chuy, Jr., Y. Hirata, Z. Wang, and K. Kosuge, "Motion control algorithms for a new intelligent robotic walker in emulating ambulatory device function," in *Proc. IEEE Int. Conf. Mechatronics Autom.*, Niagara Falls, ON, Canada, Jul. 2005, pp. 1509–1514.

[12] O. Y. Chuy, Y. Hirata, Z. Wang, and K. Kosuge, "A control approach based on passive behavior to enhance user interaction," *IEEE Trans. Robot.*, vol. 23, no. 5, pp. 899–908, Oct. 2007.

[13] W. H. Mou, M. F. Chang, C. K. Liao, Y. H. Hsu, S. H. Tseng, and L. C. Fu, "Context-aware assisted interactive robotic walker for Parkinson's disease patients," in *Proc. IEEE/RSJ Int. Conf. Intell. Robots Syst.*, Algarve, Portugal, Oct. 2012, pp. 329–334.

[14] K. Wakita, J. Huang, P. Di, K. Sekiyama, and T. Fukuda, "Human-walking-intention-based motion control of an omnidirectional-type cane robot," *IEEE/ASME Trans. Mechatronics*, vol. 18, no. 1, pp. 285–296, Feb. 2013.

[15] K. T. Song and C. Y. Lin, "A new compliant motion control design of a walking-help robot based on motor current and speed measurement," in *Proc. IEEE/RSJ Int. Conf. Intell. Robots Syst.*, St. Louis, MO, USA, Sep. 2009, pp. 4493–4498.

[16] K. T. Song and S. Y. Jiang, "Force-cooperative guidance design of an omni-directional walking assistive robot," in *Proc. IEEE Int. Conf. Mechatronics Autom.*, Beijing, China, Aug. 2011, pp. 1258–1263.

[17] K. A. Tahboub, "Natural and manmade shared-control systems: An overview," in *Proc. IEEE Int. Conf. Robot. Autom.*, Seoul, South Korea, May 2001, pp. 2655–2660.

[18] Q. Zeng, C. L. Teo, B. Rebsamen, and E. Burdet, "A collaborative wheelchair system," *IEEE Trans. Neural Syst. Rehabil. Eng.*, vol. 16, no. 2, pp. 161–170, Apr. 2008.

[19] D. Vanhooydonck *et al.*, "Adaptable navigational assistance for intelligent wheelchairs by means of an implicit personalized user model," *Robot. Auto. Syst.*, vol. 58, no. 8, pp. 963–977, Aug. 2010.

[20] T. Carlson and Y. Demiris, "Collaborative control for a robotic wheelchair: Evaluation of performance, attention, and workload," *IEEE Trans. Syst., Man, Cybern., Syst.*, vol. 42, no. 3, pp. 876–888, Jun. 2012.

[21] W. Xu, J. Huang, Y. Wang, C. Tao, and L. Cheng, "Reinforcement learning-based shared control for walking-aid robot and its experimental verification," *Adv. Robot.*, vol. 29, no. 22, pp. 1463–1481, 2015.

[22] T. Murakami, R. Nakamura, F. Yu, and K. Ohnishi, "Force sensorless impedance control by disturbance observer," in *Proc. Rec. Power Convers. Conf.*, Yokohama, Japan, 1993, pp. 352–357.

[23] S. Oh, N. Hata, and Y. Hori, "Control developments for wheelchairs in slope environments," in *Proc. Amer. Control Conf.*, Portland, OR, USA, Jun. 2005, pp. 739–744.

[24] J. Wang and Y. Li, "Kinematics and tip-over stability analysis for a mobile humanoid robot moving on a slope," in *Proc. IEEE Int. Conf. Autom. Logistics*, Qingdao, China, Sep. 2008, pp. 2426–2431.

[25] K. T. Song and K. T. Huang, "Slope surface compliant motion control design of a walking help robot," in *Proc. CACS Automat. Control Conf.*, Taipei, Taiwan, 2009.

[26] K. T. Song and L. H. Sheen, "Heuristic fuzzy-neuro network and its application to reactive navigation of a mobile robot," *Fuzzy Sets Syst.*, vol. 110, no. 3, pp. 331–340, 2000.

[27] K. T. Song and S. Y. Huang, "Mobile robot navigation using sonar direction weights," in *Proc. IEEE Int. Conf. Control Appl.*, Taipei, Taiwan, Sep. 2004, pp. 1073–1078.

[28] K. T. Song and J. Y. Lin, "Behavior fusion of robot navigation using a fuzzy neural network," in *Proc. IEEE Int. Conf. Syst. Man*, Taipei, Taiwan, Oct. 2006, pp. 4910–4915.

[29] *LMS1xx Laser Measurement Sensors*. accessed on Jul. 6, 2015. [Online]. Available: http://www.sick.com/us/en-us/home/products/product_news/laser_measurementsystems/Pages/lms100.aspx